Monatshefte für Chemie 131, 117–129 (2000)

Monatshefte für Chemie
Chemical Monthly

Printed in Austria

Kinetics of the Oxidation of Tartrazine with Peroxydisulfate in the Presence and Absence of Catalysts

Mohamed A. Salem[1,*] and **Ali H. Gemeay**[2]

[1] Department of Chemistry, Faculty of Science, University of Qatar, Doha, Qatar
[2] Department of Chemistry, Faculty of Science, Tanta University, Tanta, Egypt

Summary. The food dye tartrazine is oxidized with peroxydisulfate in the absence and in the presence of Ag(I) and Fe(III) catalysts. In the absence of these metal ions, the reaction shows second-order kinetics, first-order in each of the reacting species. With the Ag(I) ion in the medium the reaction proceeds considerably faster, but still follows second-order kinetics. The reaction rate depends on the concentration of Ag(I) and $S_2O_8^{2-}$, but is independent of the concentration of the substrate. When Fe(III) acts as the catalyst, a marked enhancement in the reaction rate is observed, and the reaction proceeds through two parallel pathways, the catalyzed and the noncatalyzed. The catalyzed path follows third order kinetics, being first-order in substrate, oxidant, and catalyst concentration. Mechanisms of the noncatalyzed as well as the Ag(I) and Fe(III) catalyzed reaction systems are proposed.

Keywords. Dyes; Homogeneous catalysis; Oxidation kinetics; Peroxydisulfate; Tartrazine.

Introduction

Several synthetic dyes have been extensively used as color additives in food and beverages [1], among them tartrazine (**1**) which is an azo dye. Tartrazine is one of the nine certified colors approved by the FDA classified as FD & C yellow 5. The genotoxicity of these products has been studied [2,3]. The decolorization process of the dye has been attributed to additives like baking soda and sucrose [4]. When carbonated beverages are packed in cans rather than glass bottles, corrosion of can material may occur. Certified dyes themselves are not corrosive, but they act as

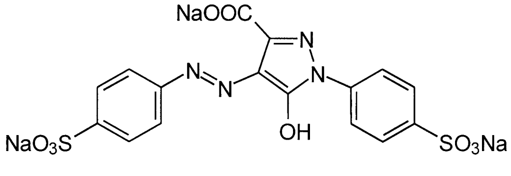

1

---

[*] Corresponding author

depolarizers which facilitate the attack of other ingredients such as acids and CO_2 on the metal [5]. Peroxydisulfate ($S_2O_8^{2-}$), on the other hand, is an environmentally benign, safe, and readily accessible oxidizing agent with a redox potential of $E(S_2O_8^{2-}/2SO_4^{2-}) = +2.05$ V. This potential exceeds that of Ag^{2+}/Ag^+ (+1.987 V), Co^{3+}/Co^{2+} (+1.84 V), H_2O_2 (+1.8 V), MnO_4^- (+1.7 V), oxygen (+1.2 V), and Fe^{3+}/Fe^{2+} (+0.77 V). Because the oxidation potential of $S_2O_8^{2-}$ is high enough, oxidation of organics is a virtually omnivorous process. Many studies have been devoted to the reaction between $S_2O_8^{2-}$ and organic substrates. These include aromatic secondary and tertiary amines and azo compounds [6, 7]. Some of these reactions are slow unless a suitable catalyst is present [8, 9]. Metal ions of variable oxidation states enhance the decomposition of peroxydisulfate in a peroxydisulfate-substrate redox system which accelerates the oxidation of the organic component [10]. A literature survey revealed that the oxidation of tartrazine with $S_2O_8^{2-}$ has not yet been studied. Therefore, this paper deals with the kinetics of this oxidation in the absence and in the presence of variable-valence metal ions as homogeneous catalysts.

Results and Discussion

Noncatalyzed oxidation

When peroxydisulfate was added to a tartrazine (**1**) solution, the absorbance of **1** decreased with time, and a gradual loss of color was observed (Fig. 1). Although the $[S_2O_8^{2-}]/[\mathbf{1}]$ ratio was *ca.* 1650, the absorbance decreased slowly. The absorbance *vs.* time data were found to fit the expression $A_t = A_o e^{-k_o t}$, which is characteristic of first-order kinetics in [**1**]. The *pseudo*-first-order rate constant k_o was determined from

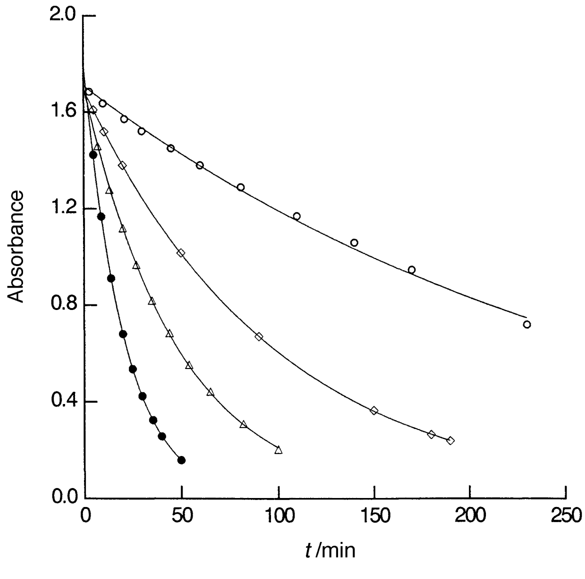

Fig. 1. Decrease in absorbance of **1** with time during its noncatalyzed oxidation with $S_2O_8^{2-}$ at various temperatures; ○: 35°C, □: 40°C, △: 45°C, ●: 50°C; [**1**] = 6.66×10^{-5} *M*, $[S_2O_8^{2-}] = 6.67 \times 10^{-2}$ *M*

Table 1. Activation parameters for the catalyzed and noncatalyzed reaction; $[\mathbf{1}] = 6.67 \times 10^{-5}\,M$, $[S_2O_8^{2-}] = 6.67 \times 10^{-1}\,M$, $[Ag(I)] = 3.33 \times 10^{-5}\,M$, $[Fe(III)] = 3.33 \times 10^{-5}\,M$

T / °C	k_o / $10^{-3} \cdot min^{-1}$	E / $kJ \cdot mol^{-1}$	$\Delta H^{\#}$ / $kJ \cdot mol^{-1}$	$\Delta G^{\#}$ / $kJ \cdot mol^{-1}$	$\Delta S^{\#}$ / $J \cdot mol^{-1} \cdot K^{-1}$
Noncatalyzed reaction					
35	3.59				
40	10.29	140.81	138.19	88.63	150
45	20.99				
50	48.10				
Ag(I)-catalyzed reaction					
35	52.48				
40	93.53	83.24	80.64	83.33	−10
45	134.56				
50	204.82				
Fe(III)-catalyzed reaction					
25	15.6				
30	27.1	58.48	55.94	47.41	20
35	39.6				
40	51.6				

the corresponding ln (absorbance) *vs.* time plot. The plot was linear for three half-lives, verifying the equation $\ln A_t = \ln A_o - k_o t$. Since the order of reaction with respect to $S_2O_8^{2-}$ is unity in such type of redox reactions [8], the rate law can be expressed as

$$-d[\mathbf{1}]/dt = k[\mathbf{1}][S_2O_8^{2-}] = k_o[\mathbf{1}] \quad (1)$$

The k_o values were determined at various temperatures and used to estimate the activation parameters (Table 1).

The dependence of the *pseudo*-first-order rate constant on the *pH* value is shown in Fig. 2. The rate constant increases as the *pH* rises from 2.6 to 10.5. This indicates that the $S_2O_8^{2-}$ ion favors the attack of the unprotonated **1** species that are present in the basic form. The more acidic medium causes protonation of the substrate which then becomes less vulnerable to react with peroxydisulfate.

Ag(I) Catalyzed oxidation

Oxidation of **1** with $S_2O_8^{2-}$ was studied in the presence of Ag(I) as catalyst. Addition of Ag(I) to the $S_2O_8^{2-}/\mathbf{1}$ reaction mixture led to a rapid decrease in the absorbance of **1** with time, although $[S_2O_8^{2-}]$ was present only in 400-fold excess of [**1**], which is much less compared with that applied in the absence of Ag(I). The effect of [Ag(I)] on the reaction rate was investigated by maintaining both dye and oxidant concentration constant. The plot of the initial rate (v_o) *vs.* [Ag(I)] was found to be linear (correlation coefficient: 0.99) with intercept zero. The linearity testifies a first order dependence of rate on the catalyst concentration (Fig. 3). The slope represents the catalytic rate constant k_c with a value equal to $1475.75\,min^{-1}$. Fig. 3 also proves that the noncatalyzed path of reaction does not exist under these

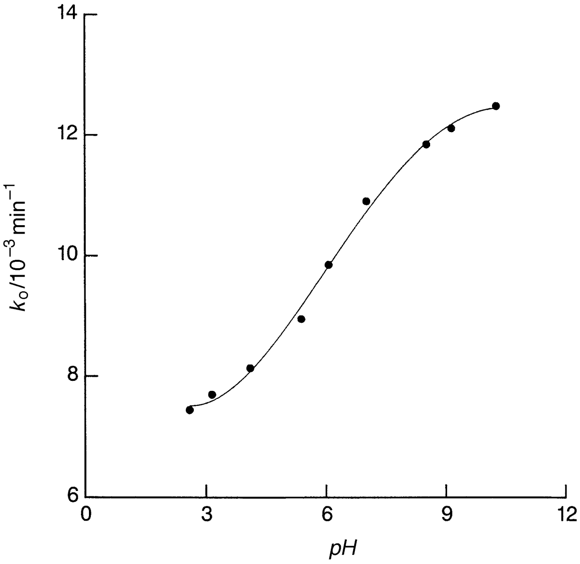

Fig. 2. Changes of the rate constant with *pH* for the noncatalyzed reaction of **1** with $S_2O_8^{2-}$; [**1**] = 6.66×10^{-5} *M*, [$S_2O_8^{2-}$] = 6.67×10^{-2} *M*, *T* = 40°C

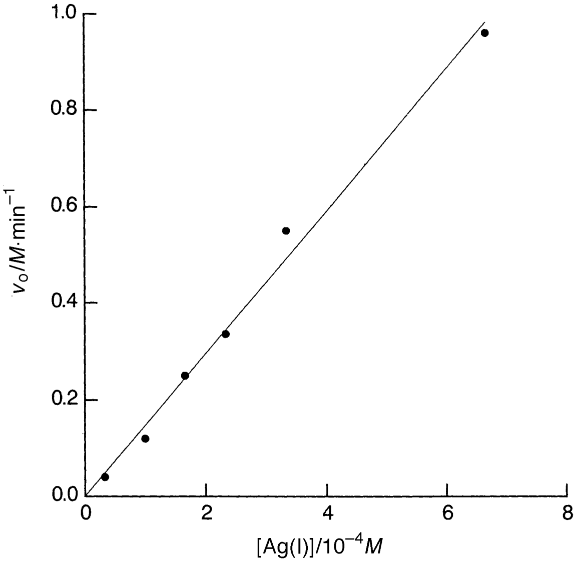

Fig. 3. Effect of Ag(I) concentration on the reaction rate of the Ag(I)-catalyzed reaction of **1** with $S_2O_8^{2-}$; [**1**] = 6.66×10^{-5} *M*, [$S_2O_8^{2-}$] = 1.67×10^{-2} *M*, *T* = 30°C

conditions. This may be attributed to the high catalytic activity of Ag(I) and the slow oxidation process encountered the absence of catalyst ion. Moreover, when the absorbance of unoxidized substrate in the presence of Ag(I) was plotted against time, a linear relationship (not shown) obeying the equation $A_t = A_o - k_o t$ was obtained when the concentration of Ag(I) was in the range of $0.33 - 3.3 \times 10^{-4}$ *M*. These findings confirm the zero-order kinetics of tartrazine species.

Table 2. Effect of the allyl acetate radical trap on the reaction rate; $[\mathbf{1}]=6.6\times10^{-5}\,M$, $[S_2O_8^{2-}]=6.67\times10^{-2}\,M$, $[\mathrm{Ag(I)}] = 3.3\times10^{-5}\,M$, $[\mathrm{Allylacetate}] = 1.23\times10^{-4}\,M$, $T = 40°\mathrm{C}$

Reaction system	$\frac{k_0}{10^{-2}\,\mathrm{min}^{-1}}$
$\mathbf{1} + S_2O_8^{2-}$	1.03
$\mathbf{1} + S_2O_8^{2-}$ + allyl acetate	0.17
$\mathbf{1} + S_2O_8^{2-} + Ag^+$	6.10
$\mathbf{1} + S_2O_8^{2-} + Ag^+$ + allyl acetate	4.30

In order to study the effect of oxidant concentration on the reaction rate, the measurements were carried out at a fixed concentration of both the substrate ($6.66\times10^{-5}\,M$) and the catalyst ($1\times10^{-4}\,M$) and at variable concentrations of $S_2O_8^{2-}$. A plot of ν_o *vs.* $[S_2O_8^{2-}]$ is a straight line passing through the origin with a correlation coefficient of 0.999. It fits the relation $\nu_o = 3.15\cdot[S_2O_8^{2-}]$ and confirms a first-order dependence of the rate on the oxidant concentration.

Since the reaction rate depends on the concentration of Ag(I) and $S_2O_8^{2-}$ and is independent of the concentration of **1**, the rate law will be

$$-\mathrm{d}[\mathbf{1}]/\mathrm{dt} = k[S_2O_8^{2-}][\mathrm{Ag(I)}] = k_c[\mathrm{Ag(I)}] \tag{2}$$

The effect of the addition of allyl acetate as a free-radical trapping agent [11] on the rate of the catalyzed and noncatalyzed oxidation of **1** was investigated. The results obtained are given in Table 2. The rate constant decreases in presence of allyl acetate in the medium. This provides good evidence that the $SO_4^{\cdot-}$ radical is generated and contributes significantly to the oxidation process of the reducing substrate.

The effect of temperature on the rate of the Ag(I) catalyzed oxidation of **1** was studied to allow calculation of the activation parameters. The temperature was increased in intervals of 5°C in the range of 30–50°C. The derived activation parameters are listed in Table 1. The activation energy of the Ag(I) mediated reaction is substantially lower than that of the Ag(I)-free reaction. This justifies that the Ag(I) ion acts as a superior catalyst for the oxidation. In absence of the catalyst, the reaction is associated with higher E and lower k_o values. This indicates that **1** is relatively stable against electrophilic attack by $S_2O_8^{2-}$ compared with the situation of the catalyzed system. Furthermore, Table 1 shows that the activation process is enthalpy controlled since the enthalpy is greater for the slower (noncatalyzed) reaction [12].

The dependence of the reaction rate upon the ionic strength was evaluated by addition of a neutral salt (K_2SO_4). Figure 4 illustrates a plot of $\ln k_o$ as a function of $I^{1/2}/(1+I^{1/2})$ where I is the ionic strength. The rate constant decreases linearly with increasing ionic strength (correlation coefficient: 0.986). It obeys the *Brönsted-Bjerrum* equation ($\ln k_o = \ln k' + 2AZ_AZ_BI^{1/2}/(1+I^{1/2})$) with a slope of $-2AZ_AZ_Bk'$ is the rate constant at zero ionic strength, Z_A and Z_B are the algebraic charge numbers of the two reacting species, and A is a constant that equals 0.509×2.303 for water at 25°C. The slope yields a value of -1.6 for Z_AZ_B. Since **1**

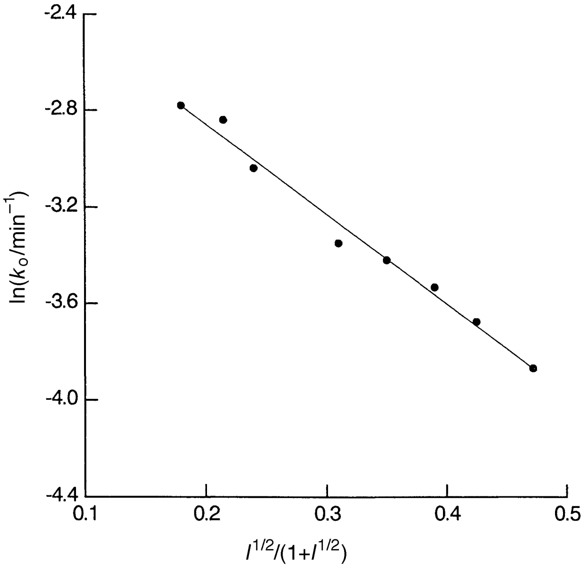

Fig. 4. Effect of ionic strength on the rate constant of the Ag(I)-catalyzed reaction of **1** with $S_2O_8^{2-}$; [**1**] = $6.66 \times 10^{-5}\,M$, $[S_2O_8^{2-}] = 1.67 \times 10^{-2}\,M$, $[\text{Ag(I)}] = 1.66 \times 10^{-4}\,M$, $T = 30°\text{C}$

exists initially as a neutral molecule, the oxidation process may likely be explained by a rate-determining reaction involving two species of opposite charges, possibly $S_2O_8^{-2}$ and Ag(I).

Fe(III) Catalyzed Oxidation

When Ag(I) is replaced by Fe(III), the absorbance of **1** declines rapidly with time (Fig. 5). Plots of ln (absorbance) *vs.* time (not shown) afford straight lines with negative slopes over the entire range of the Fe(III) concentration depicted in Fig. 5, indicating first-order kinetics in substrate concentration.

The effect of [Fe(III)] on the reaction rate was investigated. The initial rate rises with [Fe(III)] as is easily inferred from Fig. 6. This is consistent with the rate observed in the presence of Ag(I) (see Fig. 3). The plot in Fig. 6 is a straight line (correlation coefficient: 0.999) with a gradient equals to the catalytic rate constant ($1711.1\,\text{min}^{-1}$). The *y*-intercept ($0.034\,M \cdot \text{min}^{-1}$) agrees within experimental error with the rate obtained in an experiment without catalyst. Such a linear plot is characteristic of a first order dependence of the rate upon [Fe(III)] and thus indicates that the reaction proceeds through two parallel routes (catalyzed and noncatalyzed). When the *pseudo*-first-order rate constant was determined at variable concentrations of $S_2O_8^{2-}$ in the presence of Fe(III), a linear plot (correlation coefficient: 0.998) passing through the origin and obeying the equation $k_o = 0.32[S_2O_8^{2-}]$ was obtained (Fig. 7). This provides good evidence for a first-order dependence of the rate on $[S_2O_8^{2-}]$. According to these findings, the rat law can be represented by

$$-d[\mathbf{1}]/dt = k[\mathbf{1}][S_2O_8^{2-}] + k_{\text{cat}}[\mathbf{1}][S_2O_8^{2-}][\text{Fe(III)}] \qquad (3)$$

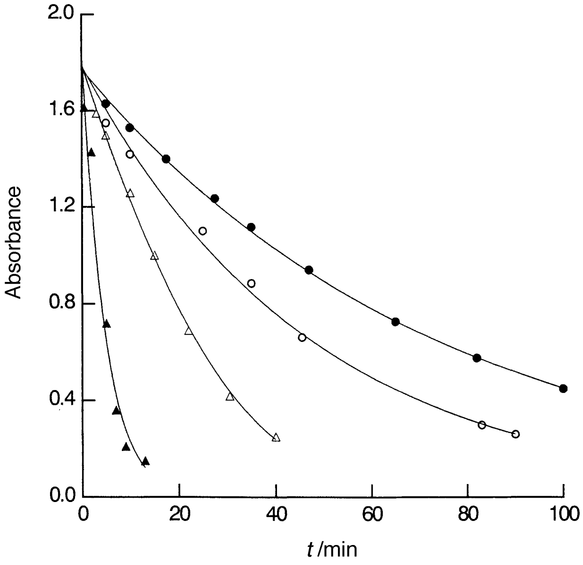

Fig. 5. Kinetic curves at various Fe(III) concentrations for the Fe(III)-catalyzed reaction of **1** with $S_2O_8^{2-}$; ●: $0.33 \times 10^{-5}\,M$, ○: $1.67 \times 10^{-5}\,M$, △: $3.3 \times 10^{-5}\,M$, ▲: $3.3 \times 10^{-4}\,M$; [**1**] = $6.66 \times 10^{-5}\,M$, $[S_2O_8^{2-}] = 6.67 \times 10^{-2}\,M$, $T = 40°C$

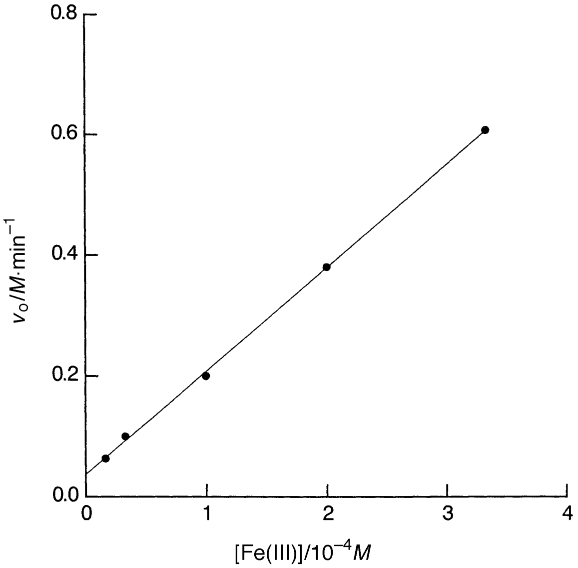

Fig. 6. Initial reaction rate as a function of [Fe(III)] (conditions as in Fig. 5)

Table 3 shows the effect of allyl acetate on the rate of the oxidation of **1** with $S_2O_8^{2-}$. Allyl acetate was added to the reaction mixture in the presence of Fe(III). The rate constant was found to decrease with increasing the concentration of radical trapping agent, confirming the participation of the arising $SO_4^{\cdot -}$ anion radical in the oxidation reaction.

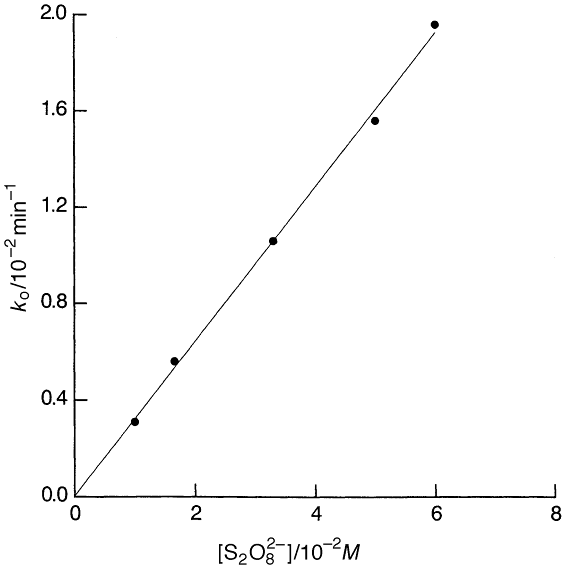

Fig. 7. Effect of $[S_2O_8^{2-}]$ on the rate constant of the Fe(III)-catalyzed reaction of **1** with $S_2O_8^{2-}$; $[\mathbf{1}] = 6.6 \times 10^{-5}\,M$, $[Fe(III)] = 1.66 \times 10^{-5}\,M$, $T = 40°C$

Table 3. Allyl acetate dependence of the Fe(III)-catalyzed oxidation of **1**; $[\mathbf{1}] = 6.6 \times 10^{-5}\,M$, $[S_2O_8^{2-}] = 6.67 \times 10^{-2}\,M$, $[Fe(III)] = 3.3 \times 10^{-5}\,M$, $T = 40°C$

$\frac{[\text{allyl acetate}]}{10^{-4}\,M}$	$\frac{k_o}{10^{-2}\,min^{-1}}$
0.0	4.81
1.23	2.43
3.70	1.95
6.17	1.50

The rate constant in the presence of Fe(III) was found to decrease linearly (correlation coefficient: 0.999) with increasing in ionic strength (Fig. 8). The slope of the plot afforded a value of -3.66 for Z_AZ_B. This value is close to -4, suggesting that a species of charge -2 reacts with a species of charge $+2$ in the rate-determining step. The predicted species are $S_2O_8^{2-}$ and Fe(II).

The activation parameters for the $\mathbf{1}/S_2O_8^{2-}/Fe(III)$ system are collected in Table 1. They cannot be compared with those obtained for the $\mathbf{1}/S_2O_8^{2-}/Ag(I)$ system as the reaction orders are different, but they confirm the catalytic action of Fe(III) relative to the noncatalyzed reaction.

Mechanism

The noncatalyzed oxidation of **1** with $S_2O_8^{2-}$ is associated with a high energy and entropy of activation (Table 1). The high values of these parameters suggest that

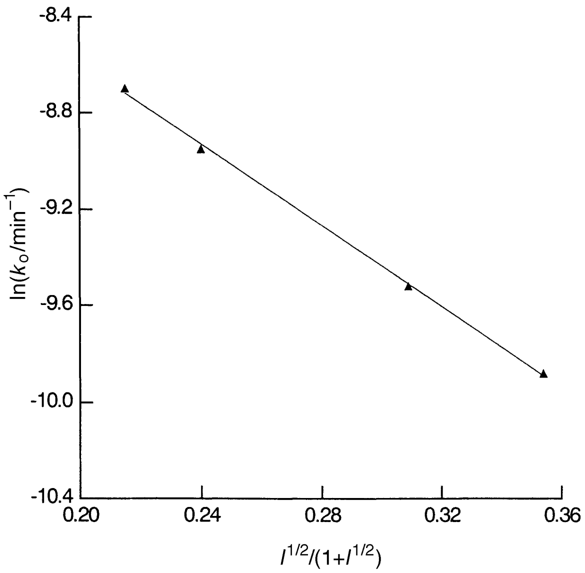

Fig. 8. Dependence of the rate constant on the ionic strength in the presence of Fe(III); $[\mathbf{1}] = 6.67 \times 10^{-5}\,M$, $[S_2O_8^{2-}] = 6.67 \times 10^{-2}\,M$, $[\mathrm{Fe(III)}] = 1.66 \times 10^{-5}\,M$

the reaction is initiated by O–O bond cleavage on $S_2O_8^{2-}$ giving rise to the active $SO_4^{\cdot-}$ radical [11,13] rather than a bimolecular interaction between **1** and the oxidant ion. This latter process always shows lower values for E and $\Delta S^{\#}$ [14]. The following is a possible mechanistic scheme describing the oxidation process.

$$S_2O_8^{2-} \xrightarrow{k_1} 2SO_4^{\cdot-} \tag{R1}$$

$$(-N{=}N-) + SO_4^{\cdot-} \xrightarrow{k_2} (-N^+-N^\cdot-) + SO_4^{2-} \tag{R2}$$

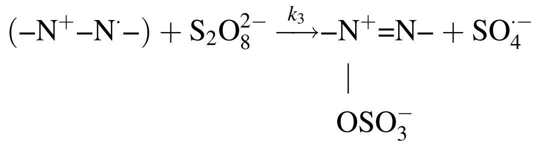

$$(-N^+-N^\cdot-) + S_2O_8^{2-} \xrightarrow{k_3} \underset{\substack{|\\ OSO_3^-}}{-N^+}{=}N- + SO_4^{\cdot-} \tag{R3}$$

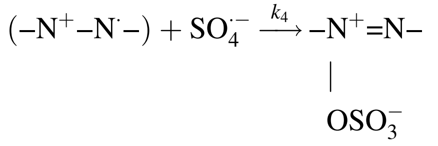

$$(-N^+-N^\cdot-) + SO_4^{\cdot-} \xrightarrow{k_4} \underset{\substack{|\\ OSO_3^-}}{-N^+}{=}N- \tag{R4}$$

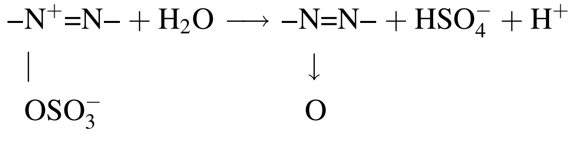

$$\underset{\substack{|\\ OSO_3^-}}{-N^+}{=}N- + H_2O \longrightarrow -N{=}\underset{\substack{\downarrow\\ O}}{N}- + HSO_4^- + H^+ \tag{R5}$$

Formation of the azoxy product in (R5) has been previously reported for the oxidation of azo-containing compounds, *e.g.* 4-(phenylazo)diphenylamine [14] and sulfacetamide [15]. $-N=N-$ and $-N^+-N^{\cdot}-$ refer to the azo center of **1** and its radical intermediate species, respectively. Assuming a steady-state concentration of $SO_4^{\cdot-}$ and $-N^+-N^{\cdot}-$, the mechanism gives the rate law

$$-d[\mathbf{1}]/dt = (k_2k_3/k_4)[\mathbf{1}][S_2O_8^{2-}] \tag{4}$$

which is consistent with the experimental rate law given in Eq. (1); k_2k_3/k_4 represents the second-order rate constant k.

When the experiment called for the addition of Ag(I), this ion was added to the substrate solution prior to the addition of $S_2O_8^{2-}$. No reaction was detected unless $S_2O_8^{2-}$ was introduced. Numerous data have been accumulated [8,9,14,15] which confirm the accelerating effect of Ag(I) and give insight into the mechanism of its catalytic action. Based on the above observations (effects of ionic strength and radical trap), it is concluded that the first step in the oxidation process involves the reaction between $S_2O_8^{2-}$ and Ag(I) ions, whereby $SO_4^{\cdot-}$ and Ag(II) are generated. An electron transfer follows between Ag(II) and the $-N=N-$ moiety of the substrate to yield the $-N^+-N^{\cdot}-$ radical intermediate. This intermediate is then further oxidized to the azoxy product. The mechanistic scheme shown below can thus be envisaged to be in line with that reported in Refs. [14,15] where the azoxy structure has been characterized by IR and MS.

$$Ag^+ + S_2O_8^{2-} \xrightarrow{k_1} Ag^{2+} + SO_4^{\cdot-} + SO_4^{2-} \tag{R6}$$

$$Ag^+ + SO_4^{\cdot-} \xrightarrow{k_2} Ag^{2+} + SO_4^{2-} \tag{R7}$$

$$Ag^{2+} + (-N{=}N-) \xrightarrow{k_3} Ag^+ + (-N^+-N^{\cdot}-) \tag{R8}$$

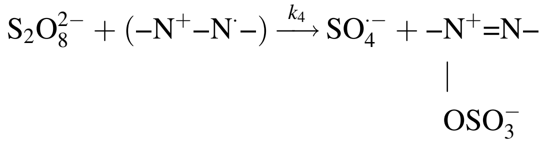

$$S_2O_8^{2-} + (-N^+-N^{\cdot}-) \xrightarrow{k_4} SO_4^{\cdot-} + \underset{\displaystyle OSO_3^-}{\underset{|}{-N^+{=}N-}} \tag{R9}$$

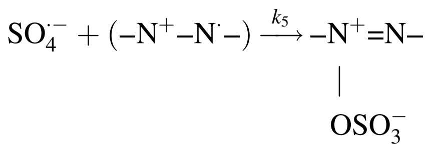

$$SO_4^{\cdot-} + (-N^+-N^{\cdot}-) \xrightarrow{k_5} \underset{\displaystyle OSO_3^-}{\underset{|}{-N^+{=}N-}} \tag{R10}$$

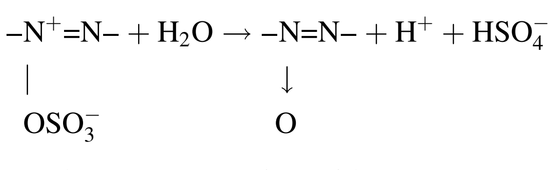

$$\underset{\displaystyle OSO_3^-}{\underset{|}{-N^+{=}N-}} + H_2O \rightarrow \underset{\displaystyle O}{\underset{\downarrow}{-N{=}N-}} + H^+ + HSO_4^- \tag{R11}$$

Application of the steady-state assumption with respect to $-N^+-N^{\cdot}-$, $SO_4^{\cdot-}$, and Ag^{2+} leads to the rate law

$$-d[\mathbf{1}]/dt = (k_1 + (k_1k_2k_4/k_5)^{1/2})[S_2O_8^{2-}][Ag(I)] \tag{5}$$

This agrees well with the observed rate law given in Eq. (2) where the second-order rate constant k represents $(k_1+(k_1k_2k_4/k_5)^{1/2})$.

With Fe(III) as the catalyst, the reaction rate increased monotically with rising Fe(III) concentration (Fig. 6). This behavior renders the Fe(III) an active catalyst for such a reaction. A probable mechanism may be described as follows.

$$\mathrm{Fe^{3+} + (-N{=}N-) \xrightarrow{k_1} Fe^{2+} + (-N^{+}-N^{\cdot}-)} \qquad \text{(R12)}$$

$$\mathrm{Fe^{2+} + S_2O_8^{2-} \xrightarrow{k_2} Fe^{3+} + SO_4^{\cdot-} + SO_4^{2-}} \qquad \text{(R13)}$$

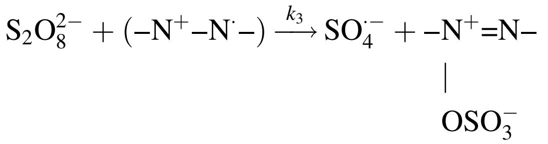

$$\mathrm{S_2O_8^{2-} + (-N^{+}-N^{\cdot}-) \xrightarrow{k_3} SO_4^{\cdot-} + \underset{\displaystyle OSO_3^{-}}{\underset{|}{-N^{+}{=}N-}}} \qquad \text{(R14)}$$

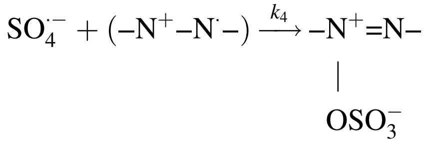

$$\mathrm{SO_4^{\cdot-} + (-N^{+}-N^{\cdot}-) \xrightarrow{k_4} \underset{\displaystyle OSO_3^{-}}{\underset{|}{-N^{+}{=}N-}}} \qquad \text{(R15)}$$

$$\mathrm{Fe^{2+} + SO_4^{\cdot-} \xrightarrow{k_5} Fe^{3+} + SO_4^{2-}} \qquad \text{(R16)}$$

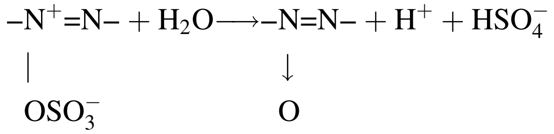

$$\mathrm{\underset{\displaystyle OSO_3^{-}}{\underset{|}{-N^{+}{=}N-}} + H_2O \longrightarrow \underset{\displaystyle O}{\underset{\downarrow}{-N{=}N-}} + H^{+} + HSO_4^{-}} \qquad \text{(R17)}$$

Support for this mechanism can be derived from (*i*) the effect of ionic strength (Fig. 8) which confirms a reaction between $\mathrm{S_2O_8^{2-}}$ and Fe(II) in (R13) (*ii*) the radical trap (Table 3) which provides evidence that the active agent $\mathrm{SO_4^{\cdot-}}$ contributes significantly to the oxidation process, and (*iii*) the formation of the azoxy product in (R17) whose structure has been characterized earlier [14]. Steady-state treatment for $\mathrm{Fe^{2+}}$, $\mathrm{SO_4^{\cdot-}}$, and $\mathrm{-N^{+}-N^{\cdot}-}$ gives the rate law

$$-\mathrm{d}[\mathbf{1}]/\mathrm{dt} = k_1(k_2k_3k_4/k_5)^{1/2}[\mathbf{1}][\mathrm{S_2O_8^{2-}}][\mathrm{Fe(III)}] \qquad (6)$$

Equation (6) is comparable with the rate of the catalyzed path of Eq. (3) where $k_1(k_2k_3k_4/k_5)^{1/2}$ represents the catalytic rate constant k_{cat}.

A comparison between the adopted mechanisms in the presence of Ag(I) and Fe(III) shows that these catalysts behave differently when they come in contact with the reacting species $(\mathbf{1} + \mathrm{S_2O_8^{2-}})$. The variation of the catalytic actions of these ions may be attributed to the oxidation state of the added ion. When Ag(I) is introduced into the reaction mixture, it is first oxidized by $\mathrm{S_2O_8^{2-}}$ forming Ag(II) (R6). This active ion is then reduced by **1** back to Ag(I) (R8) which further reacts with $\mathrm{SO_4^{\cdot-}}$ (R7) to continue the catalytic cycle. The results obtained from the ionic strength experiment clearly indicate that R6 is the initiation step of the mechanism. In contrast, Fe(III) is initially reduced by **1** to Fe(II) (R12) which is then oxidized by $\mathrm{S_2O_8^{2-}}$ to Fe(III) (R13). This ion enters the catalytic cycle to complete the reaction. (R13) is also verified by the data obtained from the corresponding ionic strength experiment.

Conclusions

The artificial food dye **1** was found to be sensitive to oxidation by $S_2O_8^{2-}$. During the oxidation there was a loss in color. The loss occurred owing to the conversion of the dye into a product which is not classified as a food additive. There is more than one effect that have impact on the rate of conversion. The conversion was higher in alkaline medium, in the presence of metal ion catalysts (Ag(I) and Fe(III)), and upon raising the temperature. The metal ion catalysts were the most responsible promoters for increasing the reaction rate. For these reasons, the environment in which **1** exists can be considered crucially for its degradation. Therefore, it can be concluded that if tartrazine contained in food is subjected to conditions resembling those discussed above during storage it is prone to oxidation which, however, may be suppressed by replacing the metal cans by a noncatalytic material such as glass.

Experimental

Materials

Tartrazine (**1**, Aldrich) was used as received. Its stock solution was prepared in distilled H_2O and was diluted to the desired concentrations. $K_2S_2O_8$ (Fluka) was recrystallized from distilled H_2O. Its solutions were immediately prepared before the measurements to avoid the change of concentration due to self-decomposition. Other chemicals were of analytical reagent grade and were used without further purification.

Kinetic measurements

Kinetics profiles were studied under *pseudo*-first-order conditions in solutions containing excess peroxydisulfate. The change in absorbance of **1** at 426 nm was monitored for 3–5 half-lives using the conventional spectrophotometric technique. The measurements were performed in a 1 cm cell on either Shimadzu 2100S or Perkin-Elmer Lambda 2S UV/Vis spectrophotometers. The cell holder temperature of the former instrument was held constant electronically by the aid of an attached Shimadzu temperature controller. With the latter machine, the temperature was adjusted by a H_2O circulation system. The *pseudo*-first-order rate constant was determined from *ln*(absorbance) *vs*. time plots according to the expression $\ln A_t = \ln A_o - k_o t$.

Acknowledgements

We thank Prof. *E. M. Ebeid* for providing a sample of **1** and Dr. *A. A. Ismail* for general discussion.

References

[1] Barbara B (1989) Farbstoffe in Lebensmitteln und Arzneimitteln, Wissenschaftliche Verlagsgesellschaft mbH, Stuttgart
[2] Combes R, Haveland-Smith R (1982) Mutat Res **98**: 101
[3] Merville MP, Decuyper J, Lopez M, Piette J, van de Vorst A (1989) Photochem Photobiol **40**: 221
[4] Mukherjee D, Mathev TV, Bhattacharjee SK, Mitra SN (1971) Res Ind **16**: 190
[5] Woodroof JG, Phillips GF (1981) Beverages Carbonated and Noncarbonated. AVT Publishing, Westport, Connecticut, p 183
[6] Sabesan A, Venkataasbramanlan N (1971) Aust J Chem **24**: 163
[7] El-Sheikh MY, Salem MA, Ismail AA, Zaki AB (1993) J Phys Org Chem **6**: 609

[8] Salem MA, El-Sheikh MY, Ismail AA, Zaki AB (1993) J Chim Phys **90**: 1201 and references therein
[9] Jonnalagadda SB, Choudary V, Bhattacharga AK (1983) J Chem Soc Perkin Trans II, 849
[10] Kislenko VN, Berlin AA, Litovchenko NV (1997) Kinetics Catalys **38**: 359
[11] Wilmarth WK, Haim A (1962) in: Edwards JO (ed) Peroxide Reaction Mechanism. Interscience, New York, p 175
[12] Salem IA (1994) Int J Chem Kinet **26**: 341
[13] House DA (1962) Chem Rev **62**: 185
[14] Salem MA, Zaki AB, Ismail AA, El-Sheikh MY (1995) Z Phys Chem **192**: 87
[15] Murty PSN, Subba-Rao PV (1977) J Indian Chem Soc **54**: 1043

Received June 28, 1999. Accepted (revised) September 27, 1999